Collisional Energy Transfer between Hot Pyrazine and Cold CO: A Classical Trajectory Study†

Cortney J. Higgins‡ and Sally Chapman*

Department of Chemistry, Barnard College, Columbia University, New York, New York 10025

Received: February 16, 2004

Vibrational energy transfer from hot pyrazine ($E' = 40\,322$ cm^{-1}) to cold CO is modeled using classical trajectories. Collisional energy transfer properties are studied as a function of the initial rotational state J' of the CO, the length of the CO, the energy E' in pyrazine, the relative kinetic energy, the temperature, isotopic substitution on pyrazine, and the intermolecular potential. The energy transfer probability function $P(E,E')$ exhibits distinct deviation from single exponential behavior. Collisions that transfer particularly large energy are associated with large amplitude out-of-plane motion of a C−H bond, imparting a kick to the departing CO. Slower collisions are particularly effective in relaxing pyrazine; faster collisions can add energy as often as they remove it. Energy transfer properties also depend on the initial rotational state of the CO. Temperature effects on $\langle E - E' \rangle$ are weak in the 200−500 K range; this results from an increase in the magnitudes of both $\langle \Delta E \rangle_{down}$ and $\langle \Delta E \rangle_{up}$. The fraction of pyrazine energy partitioned to translation increases with temperature. Decreasing the rotational temperature of pyrazine (at fixed translational temperature) decreases $-\langle E - E' \rangle$ significantly. Decreasing translational temperature (at fixed pyrazine rotational temperature) increases $-\langle E - E' \rangle$. This is in contrast to the conventional expectation, based on Landau−Teller theory. Effects of making modest changes of the intermolecular potential are also discussed.

Introduction

Understanding how energy is transferred in gas phase molecular collisions is important in many complex processes, including combustion and atmospheric chemistry. It is well-known that vibrational energy transfer in collisions is generally inefficient: even molecules with large excitation energies relax slowly.[1,2] An essential component of master equation simulations[3] is the probability $P(E,E')$ that after a single collision with a specified partner, a given molecule with energy E' will have final energy E. $P(E',E)$ is often[4] taken to be exponential in the energy gap $\Delta E = E - E'$, as predicted by the Born approximation.[5] If the downside of $P(E,E')$ is taken to be a simple exponential, $P(E,E') = A \exp(-\Delta E/\alpha)$, the parameter α, related to the average energy transfer, suffices to describe P; α generally increases with the initial excitation E'. For highly energetic molecules, those with large E', energy is lost on average, but there are collisions that transfer energy into the energized molecules. The shape of the up-side ($E - E' > 0$) of $P(E,E')$ is governed by detailed balance. In recent years it has become possible to probe in greater detail the shape of the function $P(E',E)$, with clear evidence in some cases for significant deviation from single exponential behavior. Some years ago, the term "supercollision" was coined to describe a small set of events that resulted in anomalously large values of ΔE. Supercollisions were reviewed by Oref.[6]

A number of experimental methods are used to probe the function $P(E,E')$ for highly excited molecules.[2,7] Many studies in recent years have taken advantage of the photophysics of small aromatic molecules, like benzene, perfluorobenzene, azulene, toluene, and pyrazine. Excited by UV laser, these molecules undergo prompt internal conversion, generating a well-characterized highly excited energy in the ground electronic state. Two techniques provide information about average collisional energy transfer: monitoring ultraviolet absorption (UVA), pursued by Troe and co-workers,[8−10] and infrared fluorescence (IRF), investigated by Barker and co-workers.[7,11−25] A technique developed more recently in Göttingen,[26,27] kinetically controlled selective ionization (KCSI), provides complete $P(E,E')$ distributions. Recently Nilsson and Nordholm[28,29] have used their partially ergodic collision theory[30−32] to model several systems studied by KCSI. An important result of these studies is the fact that a relatively simple statistical theory—one that allows energy redistribution among a reduced set of modes—reproduces the deviation from simple exponential behavior of the $P(E,E')$ functions.

All these methods monitor in some way the energy of the hot excited polyatomic. A complementary technique, developed in Flynn's lab at Columbia,[33−40] monitors the cold collision partner. A very narrow diode laser probes the nascent population of the ro-vibronic states of the small molecule after a single collision. For those nascent states that lack significant thermal population, the diode laser provides complete product information, since the laser is sufficiently narrow that the Doppler width of the ro-vibrational line gives the postcollision translational energy. With some modeling, the $P(E,E')$ function (or at least its higher energy tail) can be extracted from the experiments.[41] Extensive work has been carried out studying relaxation of hot pyrazine by collision with CO_2;[34−39,42−46] more recent studies have investigated cold collision partners CO,[40,47] H_2O,[48,49] and DCl.[50]

There is a long history of using classical trajectory methods to explore these systems: major contributions have been made

† Part of the special issue "Richard Bersohn Memorial Issue".

* To whom correspondence should be addressed. E-mail address: schapman@barnard.edu.

‡ Present address: Department of Civil and Environmental Engineering, Carnegie-Mellon University, Pittsburgh, PA.

10.1021/jp040140l CCC: $27.50
Published on Web 05/25/2004

TABLE 1: Pyrazine Vibrational Frequencies (cm^{-1})

mode	sym	expt[a]	calcd	d_4[b]	mode	sym	expt[a]	calcd	d_4[b]
6a	A_g	601	589	575	8a	A_g	1579	1585	1542
6b	B_{3g}	698	673	650	7b	B_{3g}	3062	3041	2242
1	A_g	1015	1003	892	13	B_{1u}	3015	3042	2251
12	B_{1u}	1019	1011	868	20b	B_{2u}	3069	3055	2264
15	B_{2u}	1063	1075	839	2	A_g	3053	3060	2275
18a	B_{1u}	1135	1139	1018	16b	B_{3u}	417	264	212
9a	A_g	1235	1241	991	16a	A_u		393	343
14	B_{2u}	1335	1314	1246	4	B_{2g}	755	484	385
3	B_{3g}	1353	1356	1032	10a	B_{1g}	925	971	758
19b	B_{2u}	1413	1425	1333	17a	A_u		1036	862
19a	B_{1u}	1484	1486	1341	11	B_{3u}	785	1250	1104
8b	B_{3g}	1522	1528	1509	5	B_{2g}	976	1368	1264

[a] Reference 72. [b] Column d^4 shows the calculated frequencies for deuterated pyrazine. The final seven values are the out-of-plane modes.

by Gilbert, Lim and co-workers,[51−56] Lenzer, Luther, and co-workers,[57−60] and Bershtein, Oref and co-workers,[61−67] and others.[68] In many studies, the collision partner is a rare gas atom, but there have been polyatomic partners as well: benzene−benzene,[59] azulene−N_2 and pyrazine−pyrazine,[69] and pyrazine−CO_2, and pyrazine−*n*-propane.[60] It is standard to use pairwise additive functions to describe the intermolecular potential; Lennard-Jones (12−6) interactions are used most frequently, but other forms, such as exp-6, have also been explored.[51−53] Most commonly, the Lennard-Jones (LJ) parameters are determined starting with atom−rare gas parameters, scaling them to obtain a spherically averaged interaction potential with the desired size σ and interaction strength ϵ.[53]

In this paper we report a classical trajectory study of the pyrazine−CO system. The interaction potential is a sum of pairwise Lennard-Jones terms, but the parameters were determined by fitting to ab initio calculations. We compare our results to recent experiments in the Flynn lab.[40,47] A preliminary report of the work, hereafter called paper I,[70] includes more details about the potential.

Methods

The VENUS96 classical trajectory program, with some modifications, was used for the dynamics.[71] The potential energy function was a sum of intramolecular functions for pyrazine and CO and an intermolecular function, taken as a sum of atom−atom Lennard-Jones 12−6 terms. Pyrazine was modeled harmonically in valence coordinates: the force constants were from Billes.[72,73] The harmonic force field includes both diagonal and off-diagonal terms for in-plane stretch and bend coordinates; out-of-plane wags and torsions have diagonal terms only. Since pyrazine in our simulations has significant excitation, we found it necessary to add some extra terms to the potential to prevent unphysical motions. For example, exponential repulsive terms were added between H and C atoms across the ring to prevent out-of-plane excursions into the middle of the ring; without it a H atom can experience a sever cusp in the wag potential at 90°. We note that animations of anomalous trajectories are very useful in detecting such pitfalls in a simple valence harmonic potential. The calculated and experimental pyrazine vibrational frequencies are given in Table 1. The in-plane modes are quite well represented. Deviations are larger for the out-of-plane modes, but the agreement is reasonably good for the lowest frequency mode for which data is available. This is important, since low-frequency out-of-plane vibrations have been shown to play a key role in vibrational energy transfer.[64,67] The CO is modeled with a Morse potential.

Most of the calculations described below use the intermolecular potential described in paper I.[70] Using the PC-Spartan-Pro package, we calculated the interaction energy of pyrazine with CO, each frozen at its equilibrium geometry, using a 6-31G* basis set with MP2 correction. About 200 points were calculated for various orientations and directions of approach; the fitting parameters are in paper I. The potential is quite anisotropic. There is a relatively deep attraction for approach along the symmetry axis normal to the pyrazine, with shallower wells for most in-plane approaches. The anisotropy with respect to the CO orientation is not as strong, but there is some preference along most directions for approach with the C atom pointed inward. The calculated points with $E < 1$ kcal/mol were fit by least squares to pairwise LJ curves [$V(r) = C_{12}/r^{12} + C_6/r^6$] terms. The fit is reasonable but not highly precise. The resulting pairwise curves do not all have wells: in some cases the C_6 parameters are positive. The potential, spherically averaged over orientations of the two molecules (with the distances measured from the midpoint of the two molecules), has a well at $R_e = 4.90$ Å with a well depth ϵ of 230 cm^{-1} (0.656 kcal/mol). (This procedure is slightly different from that proposed by Lim[53] and implemented in the SIGMON code.[74]) The deepest well occurs when CO approaches along the symmetry axis normal to the pyrazine plane, with the C atom in ($R = 3.15$ Å, $V = -596$ cm^{-1}), while the shallowest well along a symmetry axis occurs when the O atom approaches along the N−N axis ($R = 5.62$ Å and $V = -52$ cm^{-1}).

For comparison, we considered additional intermolecular potentials. In each case the Lennard-Jones parameters were taken from the Autodock[75] molecular modeling package. The average of the potential based on the Autodock LJ curves has a well depth ϵ of 278 cm^{-1} at $R_e = 5.39$ Å. Two other potentials used scaled Autodock parameters. These potentials are more isotropic than the fitted ab initio potential.

Typically a batch of about 10 000 trajectories is calculated for a given choice of potential and initial conditions. All trajectories are initiated and terminated at 12 Å; the maximum impact parameter is 9 Å. In various cases, additional batches of trajectories were studied for impact parameters between 9 and 10 Å. For most of these large impact parameter events, the two molecules never undergo close collision: the trajectory is deflected weakly by the long-range tail of the relative potential. On rare occasions the partners are drawn into a close collision, but their effect on averaged quantities was negligible. The pyrazine molecule was given a fixed vibrational energy: zero-point plus the desired excitation. After excitation with a $\lambda =$ 248 nm UV laser and prompt intersystem crossing into S_1, pyrazine has $E' = 40\,322$ cm^{-1} (115.2 kcal/mol) vibrational energy above zero point, for a total of 56 600 cm^{-1} (161.9 kcal/mol). We did not add the small ($\sim$300 cm^{-1}) contribution due to thermal excitation. The rotational energy of the pyrazine was selected from the thermal distribution at a specified temperature. The CO diatomic collision partner's internal energy was determined quasiclassically for a specified J'; all simulations had CO vibrational energy corresponding to $v' = 0$. Translational energy was either selected from a thermal distribution for a specified temperature or was fixed at a single value. Representative trajectories were viewed using the VMD[76] package.

Although trajectory calculations can be used to generate rate constants for energy transfer that can be compared directly to experiment, it is conventional to report results in terms of average energy transfer per gas-kinetic collision. Several Lennard-Jones collision rates are defined, appropriate to different

transport phenomena.[77] Because we are comparing to their experiments, we adopt the form[78] used by the Flynn group:[35] $k_{LJ} = \pi\sigma^2 (8kT/\pi\mu)^{1/2} (2\epsilon/kT)^{1/3} \Gamma(2/3)$. (This differs by a small factor from k_{LJ} based on the $\Omega_{2,2}$ collision integral.) Lennard-Jones parameters for neat pyrazine and CO were as used by Miller and Barker.[21] The usual assumption[77] that, for the mixed system, ϵ is the geometric and σ the arithmetic mean of the neat values gives $\epsilon = 149$ cm^{-1} and $\sigma = 4.55$ Å for pyrazine−CO. For a 12−6 potential, this corresponds to $r_e = 2^{1/6}\sigma = 5.11$ Å. The spherically averaged ab initio potential has a deeper well at a shorter average distance.

Results and Discussion

Previous Work. The preliminary study[70] focused on the 248 nm excitation of pyrazine colliding with CO in $J' = 10$, near the average in a thermal rotational distribution at 300 K. In that paper, we made several observations that were in qualitative agreement with preliminary experimental results.[47] First, the downward branch of $P(E,E')$ was not described well by a single exponential: ln $P(E,E')$ vs $(E - E')$ showed clear positive curvature. Second, fitting the final CO rotational state to a thermal distribution for J from 15 to 25 gave a rotational temperature of about 500 K; for $J = 25-40$ the temperature was hotter, ∼750 K. The third key comparison was in the relationship between the final relative velocity and the rotational state of the CO. In the experiments, the Doppler width of the IR laser absorption gives the postcollision relative velocity for each CO rotational state. Velocity is observed to increase with CO rotational state. By binning the trajectory results by final J for CO and calculating average velocities in each bin, the trajectories too showed a positive correlation of velocity with final J, an increase of about 60% over the range from $J = 20$ to 35, in quite good agreement with experiment. Thus, we concluded in paper I that this potential offers a reasonable description of pyrazine−CO dynamics. However, the calculated energy transfers may be too large. Miller and Barker[21] excited pyrazine at 308 nm (32 467 cm^{-1}). Their fitted expression for $\langle\Delta E\rangle_{down}$ for collisions with CO gives 196 cm^{-1} at $E' = 32$ 467 nm. Their quadratic expression, evaluated at 40 322 cm^{-1} gives $\langle\Delta E\rangle_{down} = 199$ cm^{-1}. Extrapolating using just the linear term gives 258 cm^{-1}. Our trajectory result is substantially larger: 1023 cm^{-1}.

General Observations. In this paper, we explore systematic variation of a range of trajectory parameters. A few properties are quite insensitive to initial conditions. The change in the vibrational energy of the CO is very small: CO is very stiff, so essentially none of the zero-point vibrational energy escapes. Only a very few collisions in any sample result in $v = 1$; the probability per Lennard-Jones collision is less than $^1/_{1000}$. When the relative translation is at 300 K, most collisions, typically about 80%, are direct, exhibiting only one turning point in the relative coordinate. There is a roughly exponential distribution of the number of turning points, as shown in Figure 1. Some encounters are quite long-lived: the CO bounces off the pyrazine many times, often both rotating and migrating around the molecule before it escapes. Large ΔE events result from both direct and longer lived collisions.

A challenge in analyzing the results of trajectory calculations is an overabundance of data. A question we had hoped to explore was the mechanism for large ΔE events: do they result from a distinct subset of the collisions? After examining a large number of plots in which various initial and final parameters are correlated, we were unable to discern a pattern. Large pyrazine energy loss is seen in both direct collisions and in collisions with many turning points, in collisions with large and small impact parameters, and in collisions where the first encounter is with any of the atoms on the pyrazine. It was only when looking at individual trajectories that a pattern seemed to emerge: the trajectories with large ΔE generally showed the CO molecule in its final encounter poised above the plane of pyrazine, sitting above a H atom, which happens to execute a particularly large amplitude out-of-plane motion. While this is consistent with previous work,[64,65,67] drawing a definite conclusion from viewing a small subset of trajectories is quite risky, since the sampling is not random: there is simply no such thing as a typical collision.

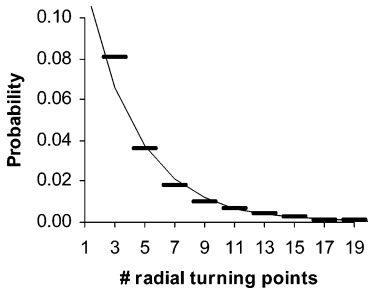

Figure 1. Distribution of turning points in the pyrazine−CO radial coordinate, for pyrazine excited with 248 nm radiation and CO ($v' = 0$, $J' = 7$). 84% of these trajectories were direct, with one turning point. Probabilities are per trajectory with $b_{max} = 9$ Å. The curve is a least-squares fit to an exponential: $P(N) = A \exp(-N/b)$ with $b = 3.54$. Similar behavior is seen for other sets of initial conditions at 300 K translational energy. Lower temperatures produced steeper distributions.

The rotation of the pyrazine was selected from a thermal distribution for a specified temperature. At $T = 300$ K, the pyrazine has an initial average rotational angular momentum of ∼40ħ. While the average change in the rotational angular momentum of pyrazine is typically small, a few ħ, transfers of 100ħ units of angular momentum or more are observed. Because of the strong coupling of rotation and vibration in a highly excited molecule, we chose not to try to report separate final vibration and rotational energies for pyrazine. There was no apparent vector correlation between the final rotational angular momentum vectors of the pyrazine and CO and only small positive correlations between the final rotation of both the pyrazine and the CO with the initial orbital angular momentum.

Figure 2 shows the (unnormalized) $P(E,E')$ distribution for collisions of hot pyrazine with CO initially in $J = 7$, which is near the maximum of the thermal distribution at 300 K. Setting $\Delta E = |E - E'|$, three fits are shown: a single exponential [$P = A \exp(-\Delta E/\alpha)$], a double exponential [$P = A_1 \exp(-\Delta E/\alpha_1) + A_2 \exp(-\Delta E/\alpha_2)$], and a stretched exponential [$P = A_s \exp(-\Delta E/\alpha_s)^y$)}, as recommended by Hold et al.[26] For simplicity the curves were fit to the downward part of the data; the resulting fit to the upward branch, as determined by detailed balance, is also shown.

As was seen previously for $J = 10$, the trajectory results deviate clearly from a single exponential, with positive curvature at larger ΔE. The stretched exponential, with $Y = 0.532$, appears to fit the data best at large ΔE, although the standard deviation of the four-parameter double-exponential fit is somewhat smaller. (Values of Y less than 1 indicate positive curvature.) However, it should be noted that obtaining consistent parameters for these fitting functions from trajectory data is problematic: when the least squares procedure properly weights the data according to its statistical uncertainty, the fit at large ΔE is often poor, since the fit may be driven by statistical fluctuations of the more probable points at small ΔE. Moreover, fits using different histogram bin sizes do not always give consistent

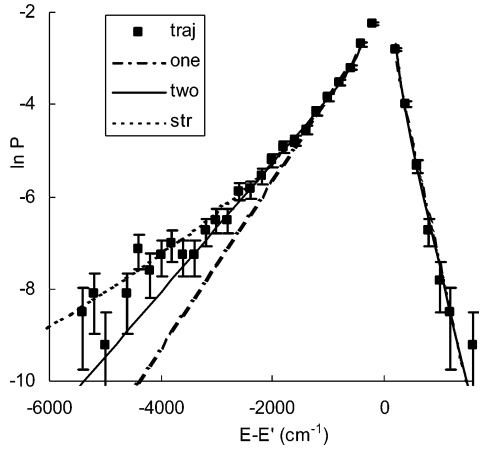

Figure 2. Energy loss ($\Delta E = E - E' < 0$) tail of the $P(E,E')$ distribution for pyrazine excited with 248 nm radiation colliding at 300 K with CO ($v' = 0$, $J' = 7$). Error bars represent one standard deviation in the statistics. Three least-squares fits are shown: single exponential, double exponential, and stretched exponential. Each function was fit to the downward data collected into 200 cm^{-1} intervals, starting at $\Delta E = -400$ cm^{-1}. The upward fit, based on detailed balancing, is also shown. Each point had unit weighting in the least-squares fit. The absolute probabilities P are per collision sampled with $b_{max} = 9$ Å and binned into 200 cm^{-1} interval, not scaled per Lennard-Jones collision.

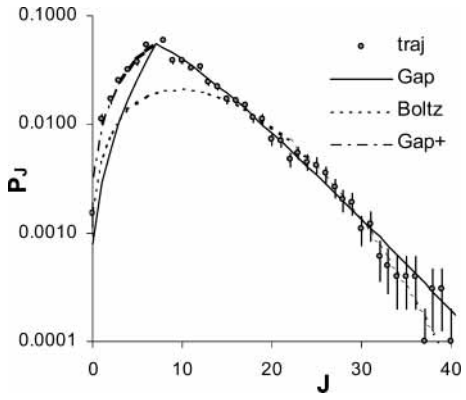

Figure 3. CO rotational distribution, for initial $J = 7$. The probabilities are per trajectory, not normalized per Lennard-Jones collision. The Boltzmann distribution is a least-squares fit for J between 15 and 25. The distribution labeled Gap is a linear least-squares fit of $\ln\{P_J/(2J + 1)\}$ vs ΔJ for ΔJ from 3 to 25. Gap+ is a separate fit for $\Delta J < 0$. Error bars indicate one standard deviation in the statistics; they are smaller than the points for smaller ΔJ.

results. The fits shown in Figure 2 are unweighted least-squares fits. Because of these problems, we do not report the $P(E,E')$ fitting parameters.

The CO rotational distribution for this same sample is shown in Figure 3. To facilitate comparison with experiment, the data for $J = 15-21$ was fit to a thermal (Boltzmann) distribution. However, this Boltzmann distribution does not fit the full range of ΔJ well. A much better fit results from using an exponential gap law in ΔJ: $P(J) = A(2J + 1)\exp^{-(J-J')/m}$. This is not surprising: exponential gap laws in ΔJ often work well for rotational energy transfer.[52,79] Such gap laws are used in the modeling to extract $P(E,E')$ curves from the Flynn group experiments.[41] (Other scaling laws are also commonly used.[3,80]) However, significantly larger values of the parameter m result from fitting the downward ($\Delta J < 0$) values of ΔJ_{CO} than from the upward ($\Delta J > 0$) ones. For $J' = 7$, m (a measure of the average ΔJ) for the upward ΔJ events is 4.5 ± 0.1 and for downward ΔJ events, 66 ± 16. Collisions that remove rotational energy from CO are significantly more probable than would be predicted by a symmetric gap law. Indeed, the probabilities $P_J/(2J + 1)$ for $\Delta J < 0$ are often nearly constant.

Effect of CO Rotation. Results showing average energy and angular momentum changes for various choices of the initial rotation of the CO (J') are given in Table 2. Figure 4 shows the trends for average energy transfer as a function of the initial CO rotational state J'. The average energy lost by pyrazine varies little, decreasing slightly in magnitude with J'. The average energy lost in downward transitions, those with $E - E' < 0$, is nearly constant. The decrease in $-\langle E - E'\rangle$ with increasing CO-(J') reflects the combination of an increasing fraction of upward collisions and an increasing average energy in the upward collisions. Despite the fact that the pyrazine is very hot, energy flow from CO rotation *into* pyrazine is significant. Energy transfer from CO rotation into pyrazine can be seen in more detail in Figure 5, showing $P(E,E')$ distributions for various J'. To avoid clutter, we have not included statistical error bars; see Figure 2 for their approximate size. As suggested by the averages, the effect of J' on the downward collisions is minimal, much less than on the upward ones.

CO final rotational distributions are shown for several J' values in Figure 6. The slope for positive ΔJ is quite insensitive to J', giving m values between 4 and 5. This is not surprising: quite some time ago, it was argued that in atom rigid-rotor collisions, each value of ΔJ is caused by a particular component of the anisotropy of the potential.[81] Subsequently it was shown that, according to the infinite order sudden approximation,[82,83] rates for the full matrix of rotational transitions J' to J may be predicted from a single column ($J' = 0-J$). This prediction has been confirmed in both quantum and classical calculations of rotational energy transfer for a number of different rotors.[84,85]

To compare with experiment, we take a thermal average over J' of these results for fixed initial J'. On the basis of the five J' sets of data presented above, the thermal averages at 300 K give $\langle E - E'\rangle$ of -544 cm^{-1}, with 314 cm^{-1} (58%) going into translation and 234 cm^{-1} into rotation of the CO. The average probability per Lennard-Jones collision of producing CO in $v = 1$ is $^1/_{2100}$. Since this is an infrequent event, this number is has large uncertainty. The measured probability[40] at 298 K is $^1/_{519}$. In the experiments, vibrational excitation of CO is accompanied by very small amounts of rotational and translational excitation. For this reason, it is argued that the mechanism is long-range dipole−dipole interaction. The intermolecular potential used in our calculation, a sum of Lennard-Jones pairs, would not describe correctly the long-range part of the potential.

On average, CO gains $3.9\hbar$ of angular momentum, pyrazine $11.4\hbar$. Using just these J' results, the initial $T = 300$ K average rotational temperature for $J = 25-30$ is 766 K. A slightly more sophisticated average can be found by forming a CO J distribution in final J by convoluting a Boltzmann average in initial J' with an exponential gap in ΔJ, assuming a constant gap parameter of 4.2. At initial $T = 300$ K, this gives a CO rotational temperature of 586 K for $J = 15-20$ and 750 K for $J = 20-30$.

Long CO. The pyrazine CO_2 system, which has been studied extensively, shows some experimental similarities to the pyrazine−CO system. For collisions resulting in no CO_2 vibrational excitation, the rotational distributions are broad, and final rotational states were observed from 58 to 82.[35] As a simple model to explore one aspect of the difference between vibrational relaxation of pyrazine by CO and CO_2, we represented CO_2 as a "long CO": CO with a doubled equilibrium bond length. All other potential parameters are unmodified. "Long CO" results are included in Table 2 and compared with normal

TABLE 2: Effect of Varying Initial CO Rotational State J' and the Length of the CO Rotor[a]

			pyrazine					CO		ΔJ		fits to rotation	
CO	J	E_{rot}	$\langle E - E' \rangle$	up	down	%d	ΔE_{trans}	ΔE_{rot}	ΔE_{vib}	CO	pyr	T_{rot} (K)	m
normal	0	0	−607	169	1023	65	243	368	−4	13.5	8.3	605 ± 137	4.7
normal	7	156	−566	186	1009	63	284	284	−2	4.9	10.6	587 ± 30	4.5
normal	10	306	−520	220	1020	60	335	190	−5	2.0	12.6	747 ± 85	4.0
normal	15	667	−473	220	942	60	295	0	−3	1.8	11.1	701 ± 50	3.8
normal	20	116 6	−372	403	1039	54	465	−97	4	−3.0	15.5	661 ± 30	4.0
long	0	0	−609	169	1002	66	235	375	−2	28.6	9.0	546 ± 44	9.0
long	7	39	−617	180	1019	67	245	377	−5	19.0	8.8	557 ± 28	9.1
long	10	76	−562	183	977	64	219	346	−2	15.0	8.0	498 ± 30	10.0
long	20	292	−583	226	1088	62	338	241	2	5.3	11.6	495 ± 16	8.7

[a] E' is 40 323 cm^{-1}. The pyrazine rotation and translational energies are selected from a 300 K distribution. Energies are in cm^{-1}. Averages are per Lennard−Jones collision. "Up" ("down") are the magnitudes of the average pyrazine energy transfers including only those with $E-E'$ greater than (less than) zero. %d is the fraction of downward collisions. Changes in J are the magnitudes of the angular momentum vectors in units of $\hbar$. Parameters are also given for fitting the corotational distributions to Boltzmann and exponential gap [$P(J) = A(2J + 1) \exp(-|J - J'|/m)$] distributions. For normal CO the Boltzmann fits were for J from 15 to 25, for long CO to J from 30 to 50. For normal CO, the gap laws were fits to ΔJ from 3 to 25, and for long CO, ΔJ from 5 to 50.

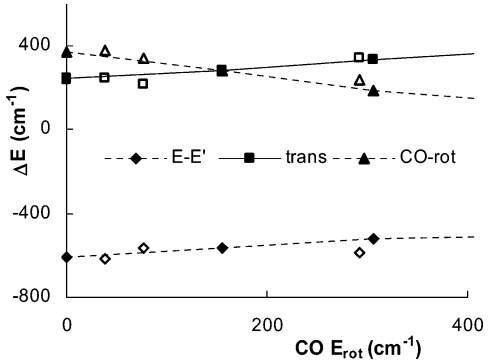

Figure 4. Effect of CO rotational energy on energy transfer. Pyrazine has $E' = 115.3$ kcal/mol (40 323 cm^{-1}) excitation in excess of zero-point energy; translational and pyrazine rotational temperatures are both 300 K. CO starts in $v' = 0$ with rotational energy as indicated. Average energy transfers are normalized per Lennard-Jones collision. The filled symbols are for normal CO, the open symbols for an artificial long CO, discussed below.

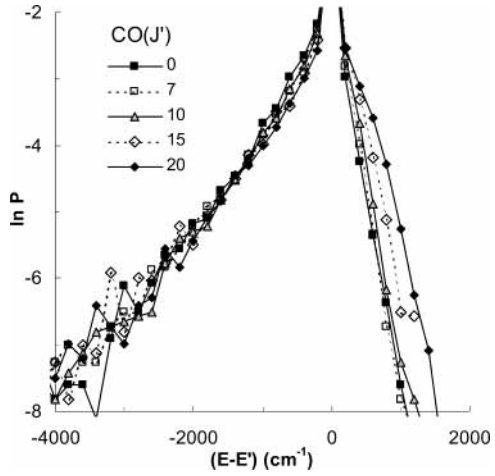

Figure 5. Energy transfer $P(E,E')$ from pyrazine with $E' = 115.3$ kcal/mol (40 323 cm^{-1}) excitation in excess of zero-point energy; translational and pyrazine rotational temperatures are both 300 K. CO is in $v' = 0$, with J' varying as indicated. The probabilities are per trajectory into a 200 cm^{-1} interval with $b_{max} = 9$ Å. The fluctuations for the low-probability events are a consequence of the statistical sampling.

CO in Figure 4. The results for average energy transfers are quite similar at initial comparable rotational energies. Average angular momenta transferred into the long CO are about a factor of 2 larger that in the normal CO and are in reasonable agreement with the pyrazine−CO_2 experiments. The final

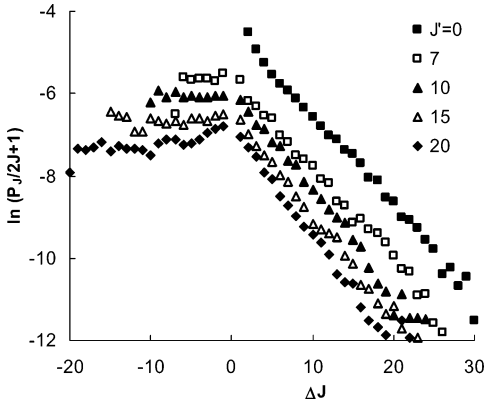

Figure 6. CO rotational distribution, for various values of initial J', as a function of ΔJ. The probabilities are per trajectory with $b_{max} =$ 9Å, not normalized per Lennard-Jones collision. The data are quite linear over a wide range in ΔJ. The slopes of the positive ΔJ branches are quite similar (see Table 2). The negative ΔJ branches have significantly smaller slopes.

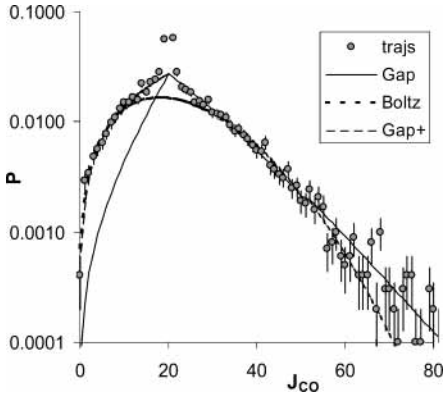

Figure 7. CO rotational distribution for "Long CO": starting in $J' =$ 20. The Boltzmann distribution, fit for $J = 30-50$, gives a temperature 495 ± 16 K. The gap law for positive ΔJ, [$P(J) = A(2J + 1) \exp(-|J - J'|/m)$], fit to $\Delta J = 5-55$, has $m = 8.75$. Error bars are one standard deviation in the statistics.

rotational distribution for $J' = 20$ is shown in Figure 7. Except for the shift in the J values, the overall appearance is quite similar to than of normal CO.

Translational Energy. When translational energy is sampled randomly from a Maxwell−Boltzmann distribution, there is a considerable range in relative translational energies. To investigate the effect of translation on energy transfer, we studied fixed translational energies of 0.5, 1.0. 2.0, and 4.0 kcal/mol

TABLE 3: Effect of Varying Initial Relative Translational Energy[a]

	pyrazine					CO		ΔJ	
E_{trans}	$\langle E - E' \rangle$	up	down	%d	ΔE_{trans}	ΔE_{rot}	ΔE_{vib}	CO	pyr
175	−612	139	986	67	425	183	4	1.8	9.6
350	−482	201	966	59	316	174	−7	1.6	11.6
700	−324	351	939	52	99	227	−2	2.5	15.2
1399	−148	659	983	49	−223	377	−6	4.7	−24.6

[a] E' is 40323 cm^{-1} and CO is initially in $J' = 10$. The pyrazine rotation and translational energies are selected from a 300 K distribution. Energies are in cm^{-1}. Averages are per Lennard-Jones collision. The changes in J are the magnitudes of the angular momentum vectors in units of $\hbar$. "Up" ("down") are the magnitudes of the average pyrazine energy transfers including only those with $E - E'$ greater than (less than) zero. %d is the fraction of downward collisions, those with $E - E'$ less than zero.

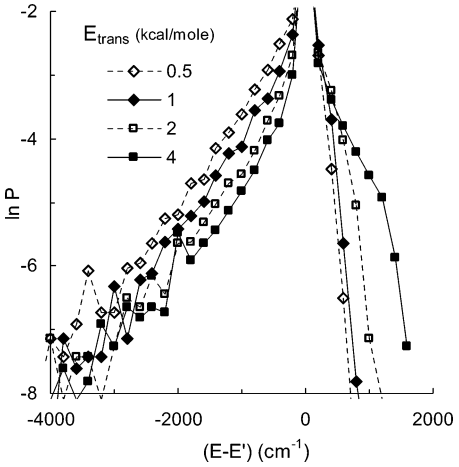

Figure 8. $P(E,E')$ for fixed translational energy, as indicated. Pyrazine has $E' = 115.3$ kcal/mol (40 323 cm^{-1}) excitation in excess of zero-point energy with 300 K rotational temperature. CO begins in $v' = 0$, $J' = 10$. The probabilities P are per collision with $b_{max} = 9$ Å, not scaled per Lennard-Jones collision.

(175, 349, 700, and 1499 cm^{-1}). The other excitations were as before: pyrazine with 248 nm vibrational excitation and rotational energy selected from a 300 K thermal distribution, and CO in $J' = 10$. Results are summarized in Table 3. Figure 8 shows the $P(E,E')$ distributions. These are clearly much more sensitive to translational energy than to CO rotation: lower energy slower collisions are significantly more effective at removing energy from pyrazine and less likely to transfer energy into pyrazine. This result may be surprising: the more common expectation for vibrational relaxation, based on Landau−Teller theory,[1] is that vibrational energy transfer increases with temperature. In Landau−Teller theory, faster motion couples more effectively to rapid vibrational motion. But hot pyrazine has a wide range of vibrational modes, all coupled with rotations, so slower collisions with multiple encounters can be very effective at relaxation.

The averages in Table 3, however, show a nearly constant average energy loss in downward collisions *per Lennard-Jones collision*: cancellation occurs because slower collisions have a larger Lennard-Jones collision cross section. (To calculate these k_{LJ} values we assumed a temperature $T = 2/3E_{trans}/k_B$). These two factors combine for the upward collisions: slower collisions, with a larger cross section, are less effective in transferring energy to pyrazine. The overall effect is quite significant: the low-energy tail of the Maxwell−Boltzmann distribution is significantly more effective in pyrazine relaxation. At higher translational energy, there are fewer long-lasting (multiple turning point) events, and large impact parameter collisions play a much smaller role: there are essentially no large ΔE collisions (collisions transferring more than 2000 cm^{-1}) for impact parameters greater that 6 Å. Observe that at 4 kcal/mol, collisions that add energy to hot pyrazine are essentially as frequent as those that relax it. The fraction of direct collisions is quite sensitive to translational energy: at 0.5 kcal/mol (175 cm^{-1}), 25% of the trajectories have at least one extra bounce in the center-of-mass coordinate and 1% bounce at least five times, while at 4 kcal/mol (1400 cm^{-1}) the collisions are essentially all direct.

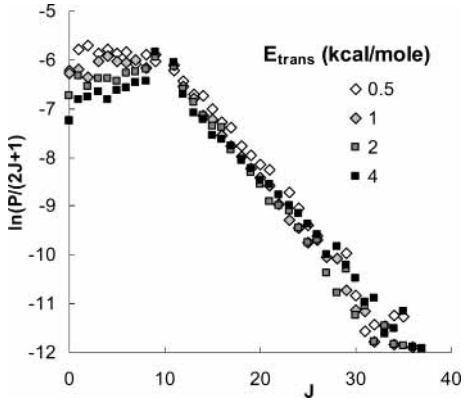

Figure 9. CO rotational state distribution for varying relative translational energy. Pyrazine has $E' = 115.3$ kcal/mol (40 323 cm^{-1}) excitation in excess of zero-point energy with 300 K rotational temperature. CO begins in $v' = 0$, $J' = 10$.

TABLE 4: Effect of Varying the Initial Pyrazine Excitation E'[a]

	pyrazine					CO		ΔJ	
E	$\langle E - E' \rangle$	up	down	%d	ΔE_{trans}	ΔE_{rot}	ΔE_{vib}	CO	pyr
36 290	−473	220	942	60	295	181	−3	1.8	11.1
40 323	−520	220	1020	60	335	190	−5	2.0	12.6
44 355	−562	212	1058	61	356	207	0	2.2	12.5

[a] CO is initially in $J' = 10$. The pyrazine rotation and translational energies are selected from a 300 K distribution. Energies are in cm^{-1}. Averages are per Lennard-Jones collision. The changes in J are the magnitudes of the angular momentum vectors in units of $\hbar$. "Up" ("down") are the magnitudes of the average pyrazine energy transfers including only those with $E - E'$ greater than (less than) zero. %d is the fraction of downward collisions, those with $E - E'$ less than zero.

The effect of translation on the rotational excitation of CO is less pronounced. For the distributions seen in Figure 9, slower collisions show some increased probability for low positive ΔJ transitions and have a significantly larger chance of removing rotational energy from the CO. The trend in the averaged values arises largely from the Lennard−Jones normalization factor.

Pyrazine Excitation. The initial pyrazine excitation, E' was also varied, with a 10% (4060 cm^{-1}) increase or decrease, again holding CO at $J' = 10$. Results are shown in Table 4. The net relaxation of pyrazine increases with pyrazine excitation, consistent with experiment.[21] This is also consistent with statistical expectations, as demonstrated in the work by Nordholm.[28,29] In this energy range, $-\langle E - E' \rangle$ is quite linear in E', with a 1.26 ± 0.03% slope. The magnitude of the average energy lost in downward transitions fits a straight line less well, but has slope 1.4 ± 0.3%. The average energy gained in upward transitions is nearly constant: in this case the increase in net energy loss comes from a larger average energy loss in downward events. The shapes of the $P(E,E')$ functions are quite similar. The partitioning of the pyrazine energy into translation

TABLE 5: Effect of Deuteration of Pyrazine[a]

	pyrazine					CO		ΔJ		$T\leftarrow V$
	$\langle E - E' \rangle$	up	down	%d	ΔE_{trans}	ΔE_{rot}	ΔE_{vib}	CO	pyr	(%)
H	−520	220	1020	60	335	190	−5	2.0	12.6	65
D	−724	198	1279	62	466	255	3	3.0	13.0	64

[a] E' is 40 323 cm^{-1} and CO is initially in $J' = 10$. The pyrazine rotation and translational energies are selected from a 300 K distribution. Energies are in cm^{-1}. Averages are per Lennard-Jones collision. The changes in J are the magnitudes of the angular momentum vectors in units of $\hbar$. "Up" ("down") are the magnitudes of the average pyrazine energy transfers including only those with $E - E'$ greater than (less than) zero. %d is the fraction of downward collisions, those with $E - E'$ less than zero.

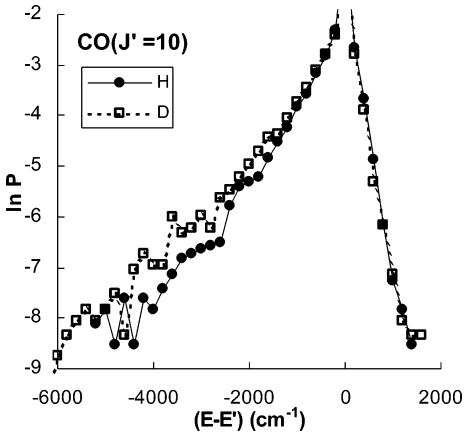

Figure 10. Effect of deuteration of pyrazine on $P(E,E')$. The vibrational energy in the pyrazine molecule is the same: 161.9 kcal/mol. CO begins in $v' = 0$, $J' = 10$. Translation and pyrazine rotation are both at 300 K.

and CO rotation is essentially constant. Miller et al.[21] used infrared fluorescence to measure pyrazine relaxation following laser excitation at 308 nm (32 460 cm^{-1}) with a number of colliders and fit their $-\langle E - E \rangle$ and $\langle \Delta E \rangle_{down}$ results to quadratic polynomials. Unfortunately, at the higher E' of this study their parabolic fits begin to decrease in E', so direct extrapolation of their pyrazine−CO results is not valid. However, a rough comparison might be made with their linear coefficients: they report a 0.79% rise with E' for $-\langle E - E' \rangle$ and 0.81% for $\langle \Delta E \rangle_{down}$.

Isotope Effects. Several studies have demonstrated that low-frequency out-of-plane wagging modes play a key role in vibrational relaxation from hot aromatics.[53,64,65,67,86] This suggests that isotopic substitution on pyrazine—replacing the H atoms with D—would enhance relaxation, since the frequencies of these doorway modes will be lower. The frequencies of the deuterated pyrazine are included in Table 1. Trajectory results for both $J' = 7$ and 10 are shown in Table 5. The total initial energy in pyrazine was held constant: the contribution from zero point energy was not adjusted. The effect is substantial: relaxation from the deuterated pyrazine is significantly enhanced. The major effect is in the downward events: the fraction increases slightly, while the average energy transferred increases a lot. This is seen in the $P(E,E')$ distributions for the two isotopomers with CO $J' = 10$, shown in Figure 10. There is a clear enhancement of the probability of collisions transferring energies from pyrazine-d_4 between 500 and 5000 cm^{-1}. The CO rotational distributions are shown in Figure 11. Deuteration enhances large positive ΔJ events while decreasing slightly the probability of CO losing rotational energy. Pyrazine-d_4 has about 2800 cm^{-1} less zero-point energy than pyrazine.[4] If the effect of total pyrazine energy on $\langle E - E' \rangle$ is ∼1.2%, as seen above,

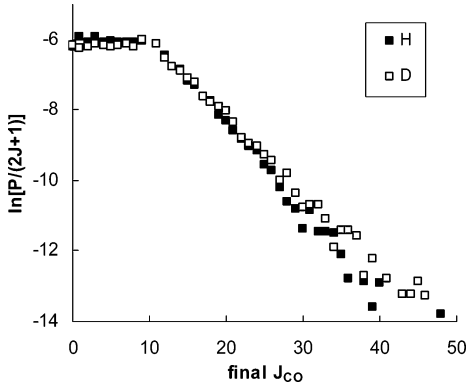

Figure 11. Effect of deuteration of the pyrazine on the CO rotational distribution. The probabilities P are per collision with $b_{max} = 9$ Å, not scaled per Lennard-Jones collision.

then adjusting the zero-point energy would decrease the size of $\langle E - E' \rangle$ by ∼33 cm^{-1}, a small fraction of the calculated effect. The large increase in the magnitude of $\langle E - E' \rangle$ seen upon deuteration of pyrazine is entirely consistent with the idea that the low-frequency modes are critical to the relaxation.

The isotope effects seen here are larger than in previous trajectory studies. Clarke and Gilbert[87] compared relaxation of azulene and azulene-d_8 colliding with helium and xenon. Deuteration enhanced the magnitude of $\langle E - E' \rangle$ and $\Delta E_{rms} = \langle E - E'^2 \rangle^{1/2}$, but only by a few percent, with a larger effect for the heavier partner. This was consistent with experiments on toluene. Lim[51] looked at toluene and toluene-d_8 colliding with Ar. He found that deuteration increased ΔE_{rms} by 13%, a value consistent with experiment.[16] He attributed this to low-frequency modes. We observe a 28% increase in ΔE_{rms} upon deuteration. While this larger effect in our results may be, in part, a consequence of the added rotational degree of freedom of the diatomic collision partner, we observed that the fraction of energy partitioned to translation did not change upon deuteration. Isotope effects in these systems are not simple: in related experiments, deuteration does not always increase the energy transfer.[18,33]

Temperature. In most of these simulations a temperature defines the initial distributions of both translational and pyrazine's rotational energy. Table 6 shows the effect of varying these temperatures, both together and separately; in each case CO starts in $J' = 10$. Of course, to compare with experiments, one would need to average over the CO rotations. For the $J' = 10$ data, overall temperature has a very minor effect on $\langle E - E' \rangle$. The magnitude of energy transfer increases in both upward and downward events, while the proportion of the two remains about the same. However, there is a systematic change in how this energy is distributed: as temperature increases, less energy is channeled into translation and more into CO rotation. In addition, increased temperature appears to enhance the energy transfer into CO rotation, at the expense of translation. At lower temperature there are more indirect collisions: those with one turning point in the center-of-mass coordinate.

When the two temperatures are adjusted independently, the small overall change in $\langle E - E' \rangle$ is seen to reflect a cancellation of two opposite trends: lower translational temperature enhances the magnitude of $\langle E - E' \rangle$ while a lower pyrazine rotational temperature reduces it. The former is consistent with the results above: slower collisions enhance relaxation. The latter effect is demonstrated more dramatically when the pyrazine rotational temperature is set to zero: the average energy transfers are reduced by more than a factor of 2. When pyrazine has no initial rotation, $\langle \Delta J \rangle_{pyr}$ is quite large. For comparison, J_{rms} in a 300 K

TABLE 6: Effect of Temperature[a]

T_{rot}−pyr (K)	T_{trans} (K)	pyrazine					CO		ΔJ		$T\leftarrow V$ (%)
		$\langle E-E'\rangle$	up	down	%d	ΔE_{trans}	ΔE_{rot}	ΔE_{vib}	CO	pyr	
200	200	−564	174	991	63	379	186	0	1.9	16.0	67
243	243	−534	187	969	62	350	189	−5	2.0	13.3	66
300	300	−520	220	1020	60	335	190	−5	2.0	12.6	65
340	340	−532	229	1040	60	327	207	−2	2.2	11.2	61
500	500	−517	314	1111	58	280	240	−3	2.7	7.3	54
243	300	−474	221	958	59	295	175	4	1.7	15.0	62
300	243	−605	183	1071	63	402	205	−2	2.1	11.6	66
0	300	−193	179	812	38	105	96	−9	0.3	48.6	55

[a] E' is 40 323 cm^{-1} and CO is initially in $J' = 10$. energies are in cm^{-1}. Averages are per lennard-Jones collision. The changes in J are the magnitudes of the angular momentum vectors in units of $\hbar$. "Up" ("down") are the magnitudes of the average pyrazine energy transfers including only those with $E - E'$ greater than (less than) zero. %d is the fraction of downward collisions, those with $E - E'$ less than zero.

TABLE 7: Varying the Intermolecular Potential Energy Surface[a]

V	J′	pyrazine					CO		ΔJ			$T\leftarrow V$ (%)
		$\langle E-E'\rangle$	up	down	%d	ΔE_{trans}	ΔE_{rot}	ΔE_{vib}	CO	pyr	%dr	
F	0	−607	169	1023	65	243	368	−4	13.5	8	80	40
F	7	−566	186	1009	63	284	284	−2	4.9	11	84	50
F	10	−520	220	1020	60	335	190	−5	2.0	13	85	65
S	0	−314	143	589	63	54	264	−4	11.5	1.6	80	17
S	7	−278	172	594	59	111	171	−4	2.9	4.0	83	40
S	10	−259	209	603	58	162	104	−7	0.6	5.3	85	63
A	0	−241	195	487	64	−23	272	−8	13.1	−1.3	71	9
A	7	−195	208	494	57	53	149	−7	2.3	1.9	77	27
A	10	−159	266	510	55	104	63	−7	−0.5	4.3	79	65
E	0	−187	166	401	62	−36	231	−8	11.7	−2.2	77	19
E	7	−134	210	412	55	23	118	−8	1.7	1.3	82	17
E	10	−109	247	423	53	74	44	−8	−0.7	3.1	84	67

[a] Potentials F, S, and E have average well depths of 230 cm^{-1}. The minimum of the spherically averaged potential for F and S is 4.90 Å; for A and E, 5.39 Å. E' is 40 323 cm^{-1} and CO is initially in $J' = 10$. The pyrazine rotation and translational energies are selected from a 300 K distribution. Energies are in cm^{-1}. Averages are per Lennard-Jones collision. the changes in J are the magnitudes of the angular momentum vectors in units of $\hbar$. "Up" ("down") are the magnitudes of the average pyrazine energy transfers including only those with $E - E'$ greater than (less than) zero. %d is the fraction of downward collisions, those with $E - E'$ less than zero. %dr is the fraction of direct collisions, those with a single turning point in the relative coordinate

TABLE 8: Lennard-Jones Parameters [$V(r) = 4\epsilon\{(\sigma/R)^{12} - (\sigma/R)^6\}$] from Autodock[a]

	σ (Å)	ϵ (kcal/mol)		σ (Å)	ϵ (kcal/mol)
C−N	3.75	0.155	O−N	3.35	0.179
C−C	4.00	0.150	O−C	3.60	0.173
C−H	3.00	0.055	O−H	2.60	0.063

[a] Reference 88.

distribution is about 45. Thus, in these collisions, pyrazine is gaining considerable rotational energy while losing internal energy overall. Decreasing the initial pyrazine rotational energy reduces the fraction of energy that is transferred to translation. The most dramatic effect of stopping pyrazine rotation is to reduce significantly the fraction of collisions with $(E - E')$ less than zero. A similar effect was seen in trajectory calculations[65] on benzene−Ar collisions: most of the collisions when $T_{rot} = 0$ K resulted in positive $\langle E - E'\rangle$.

Potential Surfaces. Table 7 compares the results above with those for different intermolecular potentials. Potential F is the fitted ab initio surface described above. Potential A uses pairwise Lennard-Jones parameters shown in Table 8, taken directly from the Autodock[75,88] molecular modeling package. In potential S, the Autodock LJ parameters were scaled uniformly to produce a spherically averaged potential with the same well depth ϵ and position r_e as potential F. The LJ σ parameters were uniformly reduced by 15% and ϵ increased by 6%. Finally, potential E scales the ϵ values to modify the spherically averaged well depth but leaves the distances fixed. In this case, the LJ ϵ parameters are decreased 17.5%.

In previous studies, it has been argued that, when the interactions are relatively strong, energy transfer depends primarily on the average well depth and position, details of the potential are less important.[53,58] However in this study, we see quite a different result. The two potentials with similar spherically averaged r_e and ϵ values, the fitted ab initio potential (F) and the scaled Autodock potential (S), exhibit quite different energy transfer. The trends with J' are quite similar, but the magnitudes are quite different: energy transfer values are significantly larger for the more anisotropic potential F. We were initially puzzled when comparing potentials A and S: the scaled potential with a shallower average well depth gave larger energy transfers. But the reason for this is simple: when reducing the overall scale of the potential (decreasing σ) it turned out that the pairwise interaction strength ϵ had to be increased to give a shallower averaged well depth. At many distances, the spherically averaged potential must combine attractive and steeply repulsive regions. This explanation is confirmed by the results on potential E, in which the pairwise σ values are the same as in potential A, but the ϵ values are less. Potential E, shallower overall, gives less energy transfer. The four potentials exhibit similar behavior in several ways: about 80% of collisions are direct, CO vibrational excitation is minimal, and for $J'(\mathrm{CO}) = 10$, about 65% of the pyrazine energy ends up in translation. All four potentials give similar dependence of $\langle E - E'\rangle$ on J': the magnitude of $\langle E - E'\rangle$ decreases, while energy transfer into translation increases. But there are differences: the unscaled Autodock potential (A) results in significantly less energy transfer. When the pairwise LJ well depth parameters are reduced, giving an average interaction strength closer to the

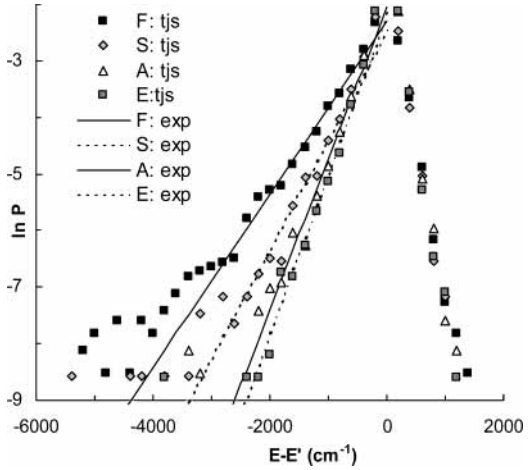

Figure 12. $P(E,E')$ varying the intermolecular potential: F, fitted to ab initio points; S, Autodock parameters scaled to have the same average ϵ and r_e as surface F; A, unscaled Autodock parameters; and *E*, autodock scaled only to have same ϵ as potential F (with distances unscaled). A single exponential is fit to each, using points with $E - E' = 400-2800$ cm^{-1}. The probabilities *P* are per collision into 200 cm^{-1} intervals with $b_{max} = 9$ Å, not scaled per Lennard-Jones collision. Refer to Figure 2 for the magnitudes of the uncertainties in the statistics.

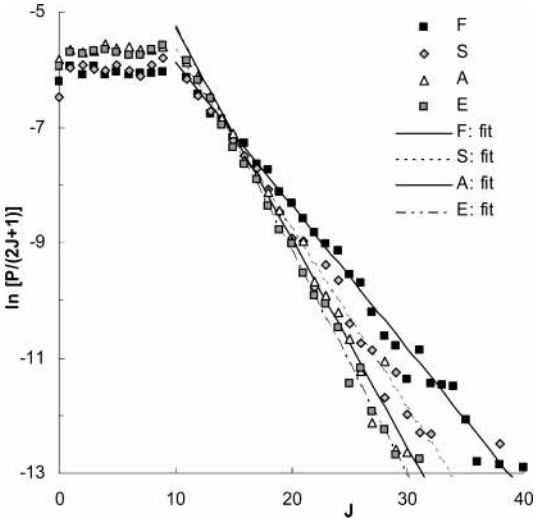

Figure 13. $P(J)$ for CO varying the intermolecular potential: F, fitted to ab initio points; S, Autodock parameters scaled to have same average ϵ and r_e as surface F; A, unscaled Autodock parameters; and *E*, Autodock scaled only to have same ϵ as potential F (with distances unscaled). The exponential gap law fit is shown for $\Delta J > 0$. The fits were obtained for $\Delta J = 3-25$. The probabilities *P* are per collision with $b_{max} = 9$ Å, not scaled per Lennard-Jones collision.

calculated values (and toward the value predicted by combining rules), the energies transferred are smaller still.

The $P(E,E')$ distributions for initial CO $J' = 10$ are shown for the four surfaces in Figure 12. As indicated by the averages, the upward ($E - E' > 0$) events show little dependence on the potential surface. The distinct pattern is in the downward branch: the ab initio surface (F) promotes many more large $-(E - E')$ events, and the deviation from single-exponential behavior is quite pronounced. Surfaces A and E have the same scale (the Lennard-Jones σ parameters are the same), but $\langle\epsilon\rangle$ is 21% larger in surface A. Interestingly, the magnitude of $\langle\Delta E\rangle_{down}$ per LJ collision is also 21% larger. It appears that potential F generates more supercollisions than the other potentials: the deviation from single-exponential behavior at large $-(E - E')$ is more pronounced. Note that we do not have adequate statistics to characterize well the large $-(E - E')$ tail for the three Autodock surfaces. However, for each there are intervals in which large $-(E - E')$ probabilities appear to be well above the exponential fit. (The lowest points shown in the figure correspond to two trajectories.)

Figure 13 shows CO rotational distributions for the four potentials, again with initial $J' = 10$. The pattern for positive ΔJ is consistent with the average energies transferred: potential F promotes the largest transitions and potential E the smallest. The pattern for negative ΔJ is interesting: all four potentials result in a nearly constant $P/(2J + 1)$, but the ordering is basically reversed: values for potential F are typically smallest, while A and E are largest.

Summary and Conclusions

Classical trajectory calculations make it possible to explore many details of collisional energy transfer that are not easily controlled in experiment. We consider collisions of highly energized pyrazine with the cold diatomic collision partner CO. Using an intermolecular potential surface constructed by fitting pairwise Lennard-Jones curves to ab initio points calculated for various orientations of the frozen partners, we have explored effects of relative translational energy, rotation of the cold partner, and temperature (of pyrazine rotation and of translation, together and separately). Slow collisions are particularly effective in relaxing pyrazine, increasing the magnitude of $\langle E - E'\rangle$. This occurs because the collisions with positive $E - E'$ are both fewer and less effective. Translational energy increases rotational excitation of the CO. Average energy transfers do not depend so strongly on the initial rotation of the CO: a decrease in $-\langle E - E'\rangle$ with J' results from a greater contribution of positive $E - E'$ events. The positive ΔJ branch of the CO rotational distributions fits an exponential gap law in ΔJ, with quite similar slopes for different values of J'. Taking a thermal average over J', we obtain $\langle E - E'\rangle$ of -544 cm^{-1}, significantly larger than would be extrapolated from lower E' infrared fluorescence (IRF) experiments.[21] (At their initial excitation energy, $E' = 32\,470$ cm^{-1}, their quadratic fit gives $\alpha = 163$ cm^{-1}.) Even though more recent KCSI experiments[27] give $-\langle E - E'\rangle$ values (for other systems) about twice as large as IRF at $E' \sim 40\,000$ cm^{-1}, it is likely that our value is still too large.

The calculated $P(E,E')$ distributions deviate distinctly from a single-exponential fit, with enhanced probability for large $-(E - E')$ events. Such supercollision tails are consistent with preliminary experimental results for this system.[47]

Deuteration of pyrazine produced larger average energy transfers, particularly enhancing the probability of larger $-(E - E')$ events. This is consistent with the assertion that the low-frequency C−H (C−D) out-of-plane wagging mode plays a critical role in relaxation. This was also observed in viewing animations of individual high ΔE collisions: a swift kick by this high-amplitude mode often characterized the last bounce in the radial motion.

We also considered different intermolecular potential surfaces. Our initial approach was to obtain the potential based on ab initio calculation. We do not claim that this method is better than that used by other workers. The level of ab initio theory (6-31G* with MP2 correction) is not expected to give very accurate results for weak intermolecular interactions, and our fitting of the ab initio points using pairwise Lennard-Jones interactions was not that precise. The fact that some of the fitted pairwise terms were purely repulsive also gives pause. The magnitudes of the energies transferred with our ab initio surface are probably too large. But our results do suggest that defining a potential simply by its spherically averaged quantities can lead

to surprises. Details of the shape of the potential, particularly for molecule−molecule energy transfer, may be more important than had been heretofore believed.

Acknowledgment. We thank Prof. George Flynn and Dr. Natalie Seiser for illuminating discussions. C.J.H. acknowledges Columbia University for a summer 2001 NSF-REU fellowship (CHE 98 20490). S. C. has benefited from many conversations over the years with Prof. Richard Bersohn.

References and Notes

(1) Houston, P. L. *Chemical Kinetics and Reaction Dynamics*; McGraw-Hill: New York, 2001.
(2) Flynn, G. W.; Parmenter, C. S.; Wodtke, A. M. *J. Phys. Chem.* **1996**, *100*, 12817.
(3) Steinfeld, J. I.; Francisco, J. S.; Hase, W. H. *Chemical Kinetics and Dynamics*; Prentice Hall: Englewood Cliffs, 1989.
(4) Pilling, M. J.; Robertson, S. H. *Annu. Rev. Phys. Chem.* **2003**, *54*, 245.
(5) Oref, I.; Tardy, D. C. *Chem. Rev.* **1990**, *90*, 1407.
(6) Oref, I. *Adv. Chem. Kinet. Dyn.* **1995**, *2B*, 285.
(7) Barker, J. R.; Brenner, J. D.; Toselli, B. M. *Adv. Chem. Kinet. Dyn.* **1995**, *2B*, 393.
(8) Damm, M.; Hippler, H.; Olschewski, H. A.; Troe, J.; Willner, J. *Z. Phys. Chem. (Munich)* **1990**, *166*, 129.
(9) Damm, M.; Deckert, F.; Hippler, H.; Troe, J. *J. Phys. Chem.* **1991**, *95*, 2005.
(10) Damm, M.; Deckert, F.; Hippler, H. *Ber. Bunsen-Ges.* **1997**, *101*, 1901.
(11) Rossi, M. J.; Pladziewicz, J. R.; Barker, J. R. *J. Chem. Phys.* **1983**, *78*, 6695.
(12) Barker, J. R.; Golden, R. E. *J. Phys. Chem.* **1984**, *88*, 1012.
(13) Forst, W.; Barker, J. R. *J. Chem. Phys.* **1985**, *83*, 124.
(14) Shi, J.; Barker, J. R. *J. Chem. Phys.* **1988**, *88*, 6219.
(15) Yerram, M. L.; Brenner, J. D.; King, K. D.; Barker, J. R. *J. Phys. Chem.* **1990**, *94*, 6341.
(16) Toselli, B. M.; Brenner, J. D.; Yerram, M. L.; Chin, W. E.; King, K. D.; Barker, J. R. *J. Chem. Phys.* **1991**, *95*, 176.
(17) Toselli, B. M.; Barker, J. R. *J. Chem. Phys.* **1991**, *95*, 8108.
(18) Toselli, B. M.; Barker, J. R. *J. Chem. Phys.* **1992**, *97*, 1809.
(19) Barker, J. R.; Toselli, B. M. *Int. Rev. Phys. Chem.* **1993**, *12*, 305.
(20) Brenner, J. D.; Erinjeri, J. P.; Barker, J. R. *Chem. Phys.* **1993**, *175*, 99.
(21) Miller, L. A.; Barker, J. R. *J. Chem. Phys.* **1996**, *105*, 1383.
(22) Miller, L. A.; Cook, C. D.; Barker, J. R. *J. Chem. Phys.* **1996**, *105*, 3012.
(23) Barker, J. R. *Ber. Bunsen-Ges.* **1997**, *101*, 566.
(24) Yoder, L. M.; Barker, J. R.; Lorenz, K. T.; Chandler, D. W. *Chem. Phys. Lett.* **1999**, *302*, 602.
(25) Yoder, L. M.; Barker, J. R. *Phys. Chem. Chem. Physics* **2000**, *2*, 813.
(26) Hold, U.; Lenzer, T.; Luther, K.; Reihs, K.; Symonds, A. C. *J. Chem. Phys.* **2000**, *112*, 4076.
(27) Lenzer, T.; Luther, K.; Reihs, K.; Symonds, A. C. *J. Chem. Phys.* **2000**, *112*, 4090.
(28) Nilsson, D.; Nordholm, S. *J. Chem. Phys.* **2002**, *116*, 7040.
(29) Nilsson, D.; Nordholm, S. *J. Chem. Phys.* **2003**, *119*, 11212.
(30) Ming, L.; Davidsson, J.; Nordholm, S. *Chem. Phys.* **1995**, *201*, 121.
(31) Ming, L.; Nordholm, S.; Schranz, H. W. *Chem. Phys. Lett.* **1996**, *248*, 228.
(32) Ming, L.; Sewell, T. D.; Nordholm, S. *Chem. Phys.* **1995**, *199*, 83.
(33) Sedlacek, A. J.; Weston, R. E., Jr.; Flynn, G. W. *J. Chem. Phys.* **1991**, *94*, 6483.
(34) Mullin, A. S.; Park, J.; Chou, J. Z.; Flynn, G. W.; Weston, R. E., Jr. *Chem. Phys.* **1993**, *175*, 53.
(35) Mullin, A. S.; Michaels, C. A.; Flynn, G. W. *J. Chem. Phys.* **1995**, *102*, 6032.
(36) Michaels, C. A.; Lin, Z.; Mullin, A. S.; Tapalian, H. C.; Flynn, G. W. *J. Chem. Phys.* **1997**, *106*, 7055.
(37) Michaels, C. A.; Mullin, A. S.; Park, J.; Chou, J. Z.; Flynn, G. W. *J. Chem. Phys.* **1998**, *108*, 2744.
(38) Sevy, E. T.; Muyskens, M. A.; Rubin, S. M.; Flynn, G. W.; Muckerman, J. T. *J. Chem. Phys.* **2000**, *112*, 5829.
(39) Sevy, E. T.; Rubin, S. M.; Lin, Z.; Flynn, G. W. *J. Chem. Phys.* **2000**, *113*, 4912.
(40) Seiser, N.; Kavita, K.; Flynn, G. W. *J. Phys. Chem. A* **2003**, *107*, 8191.
(41) Michaels, C. A.; Flynn, G. W. *J. Chem. Phys.* **1997**, *106*, 3558.
(42) Wall, M. C.; Mullin, A. S. *J. Chem. Phys.* **1998**, *108*, 9658.
(43) Wall, M. C.; Stewart, B. A.; Mullin, A. S. *J. Chem. Phys.* **1998**, *108*, 6185.
(44) Elioff, M. S.; Wall, M. C.; Lemoff, A. S.; Mullin, A. S. *J. Chem. Phys.* **1999**, *110*, 5578.
(45) Park, J.; Shum, L.; Lemoff, A. S.; Werner, K.; Mullin, A. S. *J. Chem. Phys.* **2002**, *117*, 5221.
(46) Wall, M. C.; Lemoff, A. E.; Mullin, A. S. *J. Chem. Phys.* **1999**, *111*, 7373.
(47) Seiser, N. Angular momentum constraints in the quenching of molecules with chemically significant amounts of energy: Size matters! Ph.D. Dissertation, Columbia, 2001.
(48) Fraelich, M.; Elioff, M. S.; Mullin, A. S. *J. Phys. Chem. A* **1998**, *102*, 9761.
(49) Elioff, M. S.; Sansom, R. L.; Mullin, A. S. *J. Phys. Chem. A* **2000**, *104*, 10304.
(50) Li, Z.; Korobkova, E.; Werner, K.; Shum, L.; Mullin, A. S. Private communication.
(51) Lim, K. F.; Gilbert, R. G. *J. Phys. Chem.* **1990**, *94*, 77.
(52) Lim, K. F. *J. Chem. Phys.* **1994**, *101*, 8756.
(53) Lim, K. F. *J. Chem. Phys.* **1994**, *100*, 7385.
(54) Gilbert, R. G. *Aust. J. Chem.* **1995**, *48*, 1787.
(55) Linhananta, A.; Lim, K. F. *Phys. Chem. Chem. Phys.* **1999**, *1*, 3467.
(56) Linhananta, A.; Lim, K. F. *Phys. Chem. Chem. Phys.* **2002**, *4*, 577.
(57) Lenzer, T.; Luther, K.; Troe, J.; Gilbert, R. G.; Lim, K. F. *J. Chem. Phys.* **1995**, *103*, 626.
(58) Lenzer, T.; Luther, K. *J. Chem. Phys.* **1996**, *105*, 10944.
(59) Lenzer, T.; Luther, K. *J. Chem. Phys.* **1996**, *104*, 3391.
(60) Grigoleit, U.; Lenzer, T.; Luther, K.; Mutzel, M.; Takahara, A. *Phys. Chem. Chem. Phys.* **2001**, *3*, 2191.
(61) Bernshtein, V.; Lim, K. F.; Oref, I. *J. Phys. Chem.* **1995**, *99*, 4531.
(62) Bernshtein, V.; Oref, I.; Lendvay, G. *J. Phys. Chem.* **1996**, *100*, 9738.
(63) Bernshtein, V.; Oref, I. *J. Chem. Phys.* **1996**, *104*, 1958.
(64) Clary, D. C.; Gilbert, R. G.; Bernshtein, V.; Oref, I. *Faraday Discuss.* **1996**, *102*, 423.
(65) Bernshtein, V.; Oref, I. *J. Chem. Phys.* **1997**, *106*, 7080.
(66) Bernshtein, V.; Oref, I. *J. Chem. Phys.* **1998**, *108*, 3543.
(67) Bernshtein, V.; Oref, I. *J. Phys. Chem. A* **2001**, *105*, 10646.
(68) Yoder, L. M.; Barker, J. R. *J. Phys. Chem. A* **2000**, *104*, 10184.
(69) Grigoleit, U.; Lenzer, T.; Luther, K. *Z. Phys. Chem. (Munich)* **2000**, *214*, 1065.
(70) Higgins, C.; Ju, Q.; Seiser, N.; Flynn, G. W.; Chapman, S. *J. Phys. Chem. A* **2001**, *105*, 2858.
(71) Hase, W. L.; Duchovic, R. J.; Hu, X.; Kormornicki, A.; Lim, K. F.; Lu, D.; Peslherbe, G. H.; Swamy, K. N.; Vande Linde, S. R.; Varandas, A.; Wang, H.; Wolk, R. J. VENUS96, 1996.
(72) Billes, F.; Mikosch, H.; Holly, S. *THEOCHEM* **1998**, *423*, 225.
(73) Off-diagonal terms of the force constant matrix were provided by Billes.
(74) Lim, K. F. SIGMON: An aid for the semiempirical fitting of the intermolecular potential, 1995 ed.; 1992.
(75) Morris, G. M.; Goodsell, D. S.; Huey, R.; Lindstrom, W.; Hart, W. E.; Halliday, S.; Belew, R.; Olson, A. J. Autodock 3.0, 2003.
(76) Humphrey, W.; Dalke, A.; Schulten, K. *J. Mol. Graphics* **1996**, *14*, 33.
(77) Hirschfelder, J. O.; Curtiss, C. F.; Bird, R. B. *Molecular Theory of Gases and Liquids*; John Wiley and Sons: New York, 1964.
(78) Smith, I. W. M. *Kinetics and Dynamics of Elementary Gas Reactions*; Butterworth: London, 1980; p 72.
(79) Brunner, T. A.; Pritchard, D. *Adv. Chem. Phys.* **1982**, *50*, 589.
(80) Steinfeld, J. I.; Ruttenberg, P.; Millot, G.; Fanjoux, G.; Lavorel, B. *J. Phys. Chem.* **1991**, *95*, 9638.
(81) De Jong, T.; Chu, S.-I.; Dalgarno, A. *Astrophys. J.* **1975**, *199*, 69.
(82) Goldflam, R.; Green, S.; Kouri, D. *J. J. Chem. Phys.* **1977**, *67*, 4149.
(83) Goldflam, R.; Kouri, D. J.; Green, S. *J. Chem. Phys.* **1977**, *67*, 5661.
(84) Green, S.; Chapman, S. *Astrophys. J., Suppl. Ser.* **1978**, *37*, 169.
(85) Green, S.; Chapman, S. *Chem. Phys. Lett.* **1983**, *98*, 467.
(86) Bernshtein, V.; Oref, I. *ACS Symp. Ser.* **1997**, *678*, 251.
(87) Clarke, D. L.; Oref, I.; Gilbert, R. G.; Lim, K. F. *J. Chem. Phys.* **1992**, *96*, 5983.
(88) Olson, A. J. http://www.scripps.edu/pub/olson-web/doc/autodock/parameters.html#DIFFERENCES, 2003.